

Scaling and crossover dynamics in the hyperbolic reaction-diffusion equations of initially separated components

Andrew Abi Mansour¹ and Mazen Al Ghoul^{1,2}¹*Program in Computational Science, American University of Beirut, Beirut, Lebanon*²*Department of Chemistry, American University of Beirut, Beirut, Lebanon*

(Received 16 February 2011; revised manuscript received 17 April 2011; published 5 August 2011)

In this paper we investigate the dynamics of front propagation in the family of reactions ($nA + mB \xrightarrow{k} C$) with initially segregated reactants in one dimension using hyperbolic reaction-diffusion equations with the mean-field approximation for the reaction rate. This leads to different dynamics than those predicted by their parabolic counterpart. Using perturbation techniques, we focus on the initial and intermediate temporal behavior of the center and width of the front and derive the different time scaling exponents. While the solution of the parabolic system yields a short time scaling as $t^{1/2}$ for the front center, width, and global reaction rate, the hyperbolic system exhibits linear scaling for those quantities. Moreover, those scaling laws are shown to be independent of the stoichiometric coefficients n and m . The perturbation results are compared with the full numerical solutions of the hyperbolic equations. The crossover time at which the hyperbolic regime crosses over to the parabolic regime is also studied. Conditions for static and moving fronts are also derived and numerically validated.

DOI: [10.1103/PhysRevE.84.026107](https://doi.org/10.1103/PhysRevE.84.026107)

PACS number(s): 82.20.-w, 47.70.Fw, 82.40.Ck

I. INTRODUCTION

During the past two decades, the reaction-diffusion system with initially segregated reactants has been studied theoretically [1–8], computationally [3,9–19], and experimentally [14,20–25]. Analytical studies have focused almost exclusively on one-dimensional systems that are characterized by the presence of a propagating reaction front commonly observed in various chemical [26,27] and biological [28] systems.

In their seminal paper, Gálfi and Rácz [1] were the first to study the dynamics of a diffusion-controlled system that undergoes a chemical change of the form $A + B \rightarrow C$ and with the reactants being initially separated in space such that each occupies half the length of the total system. Their results were based on the following scaling ansatz for the density functions of the reactants: $a(z,t) \sim t^{-\gamma} G_a(z)$, $b(z,t) \sim t^{-\gamma} G_b(z)$, and for the chemical rate function, $R(z,t) \sim t^{-\beta} G_R(z)$, where t is time, $z = (x - x_f)/t^\alpha$, and x_f denotes the reaction center located at the point of intersection of the reactant density profiles. They considered the diffusion coefficients to be equal ($D_A = D_B$) and argued that this does not change the scaling of the solution functions but simply modifies some unimportant features of the shaping functions of the reactants. By neglecting microscopic fluctuations, they considered a mean-field approximation for the rate $R(x,t) = a(x,t)b(x,t)$, which in turn leads to the following values for the exponents: $\alpha = 1/2$, $\beta = 2/3$, and $\gamma = 1/3$. They also showed that x_f scales as $t^{1/2}$, the width of the front w as $t^{1/6}$, and the reaction at the center $R(x_f)$ as $t^{-2/3}$. Finally, they demonstrated that for equal initial concentrations ($a_0 = b_0$) the front was static.

In a later publication, Jiang and Ebner [10] studied numerically the same system but with unequal diffusion coefficients using random walkers on a square lattice and confirmed the analytical results derived by Gálfi and Rácz in the long time regime. They also showed that the general condition for a stationary front is $a_0\sqrt{D_A} = b_0\sqrt{D_B}$. Koo and Kopelman [22] subsequently reported experimentally

similar results to those predicted by theory and simulation. Chopard and Droz [11] investigated the validity of the mean-field approximation using a cellular automata model. They showed numerically that in two dimensions the mean-field approximation is inaccurate, and found the width to scale in time as $w \sim t^{0.186 \pm 0.005}$. They concluded that microscopic fluctuations play a significant role when the reactants are not mixed efficiently as in one-dimensional systems. Cornell *et al.* [9,16] investigated the general reaction $nA + mB \rightarrow C$ and proposed that the mean-field expression is valid for $d > d_c$, where d_c is the critical dimension of the system. By imposing two antiparallel currents at the infinite boundaries, they created a steady state system with a static front and proceeded to find, using dimensional analysis, the expression of the critical dimension d_c to be equal to $2(m + n - 1)^{-1}$. Furthermore, they proposed a quasistatic approximation (QSA) which assumes that at sufficiently long times the kinetics of the front is controlled by two separate time scales: the diffusion time scale $t_J \propto (d \ln J/dt)^{-1}$, which is a characteristic of the diffusion flux J in the neighborhood of x_f , and the reaction time scale $t_R \propto w^2/D$, which is the time required for the front to equilibrate. Since in the asymptotic domain the system is effectively diffusion controlled, the approximation $t_R/t_J \ll 1$ leads to the following QSA equations for a and b : $\nabla \cdot (D_A \nabla a) = R$ and $\nabla \cdot (D_B \nabla b) = R$. From the QSA equations, they were able to derive the following general form for the mean-field scaling exponents for arbitrary stoichiometric coefficients $n, m \geq 1$: $\alpha = (n + m - 1)/2(n + m + 1)$, $\gamma = (n + m + 1)^{-1}$, and $\beta = 2(n + m + 1)^{-1}$. They also showed that the width scales in time as $w \sim t^{1/4}$, which was also observed in systems with one static and another diffusing reactant [29]. Subsequently, Krapivsky [30] used dimensional analysis to confirm and extend the previous one-dimensional results and found that for $A + B \rightarrow C$ in two dimensions the width scales in time as $w \sim t^{1/6}(\ln t)^{1/3}$ and for the reaction $2A + B \rightarrow C$, $w \sim t^{1/4}(\ln t)^{1/4}$, indicating a failure of the mean-field approximation. Similar failure of the mean-field approach was also emphasized in the work of Mai *et al.* [31,32]

on front propagation and velocity selection in autocatalytic reactions of the form $A + B \rightarrow 2A$. Using Monte Carlo simulations, they were able to show that while for $D_A > 0$, only a uniquely stable propagating front was selected and when $D_A = 0$, they found that the front's velocity and width both scale as $t^{1/2}$. Kessler and Levine [33] showed that fluctuations in the particle number are essential to understand diffusive instabilities.

Koza [6] thereafter showed that for unequal diffusion coefficients the position of the front center is determined by solving $D_A a(x_f, t) - D_B b(x_f, t) = 0$. Koza *et al.* [34] generalized the scaling theory of Gálfi and Rácz by studying the dynamics of the system for $|x - x_f| \geq \sqrt{Dt}$, which required two length scales, those of the width and diffusion. Their multiscaling theory showed that the QSA is invalid at length scales of the order of the diffusion length and found the values of the anomalous exponents to be different from those derived from a single length scaling theory.

While numerical and theoretical studies continued in the long time limit for the system $A + B \rightarrow C$, $A + B(\text{static}) \rightarrow C$ [7,35,36], and the family of reactions $nA + mB \rightarrow C$ [37,38], Taitelbaum *et al.* [2] investigated the initial time behavior of the system $A + B \rightarrow C$ using a perturbation technique centered around the parameter ϵ , the ratio of diffusion to reaction time scales. In this study, it was argued that initially the system is dominated by diffusion, which meant that $\epsilon \approx 0$. As time progressed, ϵ increased in magnitude and the nonlinear term arising from the reaction rate becomes significant. Moreover, they showed to zero order that the front initially scales in time as $x_f \sim t^{1/2}$, the width as $w \sim t^{1/2}$, and the global reaction rate as $\mathfrak{R} \sim t^{1/2}$. A first order correction was also derived, and it was shown that the correction terms for the front and the global rate are proportional to $t^{3/2}$.

In another study [3], Taitelbaum and Koza examined analytically the dynamics of the front center. The two parameters that initially played a role in the motion of the front were found to be D and r , the square root of the ratios of diffusion coefficients $\sqrt{D_A/D_B}$, and initial concentrations $\sqrt{b_0/a_0}$, respectively. The front center was shown to exhibit a point of extremum at which there was a change in the direction of motion. The conditions for the physical existence of such an extremum were $r > 1$ and $D > 1$, or equivalently $r < 1$ and $D < 1$, with D being close to 1. They related these results to the fact that initially the system dynamics were governed by diffusion, which drove the front. Only at a later stage did the chemical reaction begin to play a significant role, and asymptotically the parameter $r^{-2}D$ became the only dominant term in controlling the front dynamics. On the other hand, when $r^{-2}D = 1$ the front center was static in accordance with the results of Ebner and Jiang in the asymptotic regime [10]. These results were also supported by experiments [29].

In this study, we investigated the dynamics of front propagation in the $nA + mB \rightarrow C$ system using hyperbolic reaction-diffusion equations. All previous studies which are based on the mean-field approximation of the reaction rate used parabolic reaction-diffusion equations to describe the transport and reaction of matter where the diffusion flux J was assumed to be Fickian, that is, $J \sim \partial c / \partial x$ leading to

the well-known unphysical problem of infinite propagation in the limit $t \rightarrow 0$. To remedy this problem, an extension to Fick's law was introduced, which in turn led to hyperbolic evolution equations of the telegraphist type to limit the velocity of propagation. We showed that beyond a certain characteristic time t_c of the system, the hyperbolic equations take a perturbed form of their parabolic counterpart until asymptotically both equations converged. The dynamics of the front were controlled by the parameters D and r , in addition to the square root of the ratio of particle masses, $M = \sqrt{m_A/m_B}$. We also showed that the conditions for a static front were functions of the stoichiometric coefficients and generalized those derived in [3]. Although in this work we do not include in the description or in the model fluctuations, the effects of which might be significant on the spatiotemporal dynamics of the system [39] (also in this regard, see the most in-depth review of Kotomin and Kuzovkov [40,41]), we solely invoke the mean-field expression of the rate to extend the results derived using the parabolic reaction-diffusion equations.

II. THE MODEL

The chemical reaction under study is of the general form



where $k \in \mathbb{R}$ represents the rate constant for the forward reaction, and n and $m \in \mathbb{N}$ since the chemical reaction is assumed to be elementary. The continuity equations for the reactants can be written as

$$\partial_t a + \nabla \cdot \mathbf{J}_A = -nR, \quad (2)$$

$$\partial_t b + \nabla \cdot \mathbf{J}_B = -mR, \quad (3)$$

where R is the rate of the chemical reaction, a and b are the density functions, and \mathbf{J}_A and \mathbf{J}_B are the diffusion fluxes for the reactants of (A) and (B), respectively. The constitutive equation for the flux can be derived from extended irreversible thermodynamics [42] or from generalized hydrodynamics [43–45]. We will assume that the following linear approximation for the diffusion fluxes is adequate to describe the system:

$$\mathbf{J}_A = -D_A \nabla a - L_{AA}^{-1} \partial_t \mathbf{J}_A, \quad (4)$$

$$\mathbf{J}_B = -D_B \nabla b - L_{BB}^{-1} \partial_t \mathbf{J}_B. \quad (5)$$

L_{AA} and L_{BB} are phenomenological coefficients, while D_A and D_B are the diffusion coefficients for the reactants A and B , respectively. We also assumed that cross diffusion is absent in this system. When L_{AA} and L_{BB} become infinite, we recover Fick's first law of diffusion. By substituting the hyperbolic flux expressions (4) and (5) into Eqs. (2) and (3), and assuming that the diffusion coefficients are constants, we obtain the following reaction-diffusion equations:

$$\partial_t \phi = \mathbf{D} \Delta \phi - \mathbf{L}^{-1} \partial_{tt}^2 \phi - k\mathbf{r} - k\mathbf{L}^{-1} \partial_t \mathbf{r}, \quad (6)$$

where $\phi = (a, b)^T$, $\Delta = \nabla \cdot \nabla$ is the Laplacian, $\mathbf{D} = \text{diag}(D_A, D_B)$, and $\mathbf{L} = \text{diag}(L_{AA}, L_{BB})$ are diagonal matrices of the diffusion coefficients and the reciprocal of the

hydrodynamic relaxation times of the reactants, respectively, and $\mathbf{r} = \text{diag}(na^{n-1}b^m, ma^n b^{m-1})\phi$. The phenomenological coefficients L_{AA} and L_{BB} are related to the diffusion coefficients by the relations

$$D_A = \frac{k_B T}{L_{AA} m_A}, \quad D_B = \frac{k_B T}{L_{BB} m_B}, \quad (7)$$

where k_B is the Boltzmann constant, T is the equilibrium Kelvin temperature, and m_i is the particle mass of species i . The rate of the reaction follows the mean-field approximation

$$R(x, t) = a^n b^m. \quad (8)$$

By introducing the dimensionless variables

$$\rho_a = a/a_0, \quad \rho_b = b/b_0, \quad (9)$$

$$\zeta = x\sqrt{a_0 b_0}, \quad \tau = ta_0 b_0 \sqrt{D_A D_B}, \quad (10)$$

Eq. (6) becomes

$$\partial_\tau \rho_a = D \Delta_\zeta \rho_a - MD\kappa \partial_{\tau\tau}^2 \rho_a - nr \epsilon \rho_a^n \rho_b^m - nMDr\kappa \epsilon \partial_\tau (\rho_a^n \rho_b^m), \quad (11)$$

$$\partial_\tau \rho_b = D^{-1} \Delta_\zeta \rho_b - \kappa(MD)^{-1} \partial_{\tau\tau}^2 \rho_b - m\epsilon r^{-1} \rho_a^n \rho_b^m - m\kappa \epsilon (MDr)^{-1} \partial_\tau (\rho_a^n \rho_b^m), \quad (12)$$

where D , r , L , and M are ratios defined as

$$D = \sqrt{\frac{D_A}{D_B}}, \quad r = \sqrt{\frac{b_0}{a_0}}, \quad M = \sqrt{\frac{m_A}{m_B}}, \quad (13)$$

$$L = \sqrt{\frac{L_{BB}}{L_{AA}}} = \sqrt{\frac{D_A m_A}{D_B m_B}} = DM. \quad (14)$$

κ and ϵ are relative time scales defined as

$$\kappa = a_0 b_0 \sqrt{D_A D_B} / \sqrt{L_{AA} L_{BB}}, \quad (15)$$

$$\epsilon = ka_0^{n-3/2} b_0^{m-3/2} / \sqrt{D_A D_B}. \quad (16)$$

It is evident from Eq. (15) that κ is the ratio of hydrodynamic relaxation to diffusion time scales. Its magnitude represents the deviation from the regime described by parabolic reaction-diffusion equations, the so-called parabolic regime. Therefore, when $\kappa \rightarrow 0$, we regain the traditional parabolic reaction-diffusion equations

$$\partial_\tau \rho_a = D \Delta_\zeta \rho_a - nr \epsilon \rho_a^n \rho_b^m, \quad (17)$$

$$\partial_\tau \rho_b = D^{-1} \Delta_\zeta \rho_b - mr^{-1} \epsilon \rho_a^n \rho_b^m. \quad (18)$$

On the other hand, ϵ in Eq. (16) represents the diffusion to reaction time scales. Following the approach of Taitelbaum *et al.* [2], we perform a perturbation expansion in terms of ϵ as follows:

$$\rho_a = \sum_i \epsilon^i \rho_a^{(i)}, \quad \rho_b = \sum_i \epsilon^i \rho_b^{(i)}. \quad (19)$$

Using expansion (19) in Eqs. (11) and (12) and collecting the terms of same power in ϵ , we obtain different orders of approximations which will be studied in the coming sections.

III. ZEROth ORDER SOLUTION: INITIAL TIME BEHAVIOR

The zeroth order solution is cast in the following form:

$$\partial_\tau \rho_a^{(0)} = D \Delta_\zeta \rho_a^{(0)} - MD\kappa \partial_{\tau\tau}^2 \rho_a^{(0)}, \quad (20)$$

$$\partial_\tau \rho_b^{(0)} = D^{-1} \Delta_\zeta \rho_b^{(0)} - \kappa(MD)^{-1} \partial_{\tau\tau}^2 \rho_b^{(0)}, \quad (21)$$

which obviously reflects the fact that the system is initially dominated by diffusion as argued by Taitelbaum *et al.* [2]. The general solution of Eqs. (20) and (21) for $\rho_a^{(0)}$ can be sought using Riemann's method [46] as such:

$$\begin{aligned} \rho_a^{(0)}(\zeta, \tau) = & \frac{1}{2} \exp\left(-\frac{\tau}{2MD\kappa}\right) \left[H\left(-\zeta - \tau\sqrt{\frac{1}{M\kappa}}\right) \right. \\ & \left. + H\left(-\zeta + \tau\sqrt{\frac{1}{M\kappa}}\right) \right] + \frac{1}{4D\sqrt{M\kappa}} \\ & \times \exp\left(-\frac{\tau}{2MD\kappa}\right) \int_{\zeta-\tau\sqrt{1/M\kappa}}^{\zeta+\tau\sqrt{1/M\kappa}} \frac{I_1\left(\frac{1}{2}\alpha\sqrt{Z}\right)}{\sqrt{Z}} \\ & \times H(-\xi) d\xi + \frac{1}{4D\sqrt{M\kappa}} \exp\left(-\frac{\tau}{2MD\kappa}\right) \\ & \times \int_{\zeta-\tau\sqrt{1/M\kappa}}^{\zeta+\tau\sqrt{1/M\kappa}} I_0\left(\frac{1}{2}\alpha\sqrt{Z}\right) H(-\xi) d\xi, \quad (22) \end{aligned}$$

where I_0 and I_1 represent the modified Bessel functions of the first kind of orders 0 and 1, respectively; $Z = 1 - M\kappa\left(\frac{\zeta-\xi}{\tau}\right)^2$ and $\alpha = \tau/MD\kappa$. It is evident from Eq. (22) that the Dirichlet boundary conditions are satisfied through the following limits: $\lim_{\zeta \rightarrow -\infty} \rho_a^{(0)}(\zeta, \tau) = 1$ and $\lim_{\zeta \rightarrow \infty} \rho_a^{(0)}(\zeta, \tau) = 0$ with $\tau/\kappa \rightarrow \infty$, and by taking the following asymptotic expansion of I_0 and I_1 ,

$$I_1\left(\frac{1}{2}\alpha\sqrt{Z}\right) \simeq \frac{1}{\sqrt{\pi\alpha}} \frac{1}{Z^{1/4}} \exp\left(\frac{1}{2}\alpha\sqrt{Z}\right), \quad (23)$$

$$I_0\left(\frac{1}{2}\alpha\sqrt{Z}\right) \simeq \frac{1}{\sqrt{\pi\alpha}} \frac{1}{Z^{1/4}} \exp\left(\frac{1}{2}\alpha\sqrt{Z}\right). \quad (24)$$

In Appendix A 1 we show that asymptotically the hyperbolic equation reduces to the parabolic form. Initially, however, there is a deviation that must be taken into account.

A. The hyperbolic domain

First, we note that by taking the limit $\kappa \rightarrow 0$, we obtain from Eqs. (20) and (21), the parabolic diffusion equation with the following well-known solutions:

$$\rho_a^{(0)}(\zeta, \tau) = \frac{1}{2} \left[1 - \text{erf}\left(\frac{\zeta}{2\sqrt{D\tau}}\right) \right], \quad (25)$$

$$\rho_b^{(0)}(\zeta, \tau) = \frac{1}{2} \left[1 + \text{erf}\left(\frac{\zeta\sqrt{D}}{2\sqrt{\tau}}\right) \right]. \quad (26)$$

Moreover, the zeroth order rate function is written as

$$R_0(\zeta, \tau) = [\rho_a^0(\zeta, \tau)]^n [\rho_b^0(\zeta, \tau)]^m. \quad (27)$$

The front position ζ_f can be defined [2] as the point in space ζ such that $R(\zeta_f) = \max_{\zeta} R(\zeta, \tau)$. An alternative definition [47] considers the front position to be equal to the first moment of the reaction rate. Both definitions become equivalent once the rate assumes a Gaussian profile. For purely analytical reasons, we shall use the first definition for the parabolic front. The reaction zone is defined as the region of space such that $|\zeta - \zeta_f| \sim \tau^{1/2}$. The scaling of ζ_f for the parabolic reaction-diffusion equations was found in [2] to be $\zeta_f^p \sim \tau^{1/2}$. It is evident that the velocity of the parabolic front, $v_p \sim \tau^{-1/2}$, tends to infinity as τ approaches 0. This is a well-known problem associated with Fickian diffusion. To correct it, we take the limit $\tau/\kappa \rightarrow 0$ and use the following Taylor expansions of the Bessel integrals of I_0 and I_1 in Eq. (22):

$$I_0\left(\frac{1}{2}\alpha\sqrt{Z}\right) = 1 + O(Z), \quad (28)$$

$$I_1\left(\frac{1}{2}\alpha\sqrt{Z}\right) = \frac{1}{4}\alpha\sqrt{Z} + O(Z^{3/2}). \quad (29)$$

The density profiles of the reactants in the reaction zone can then be written as

$$\rho_a^{(0)}(\zeta, \tau) \simeq \frac{1}{2} + \frac{1}{4D\sqrt{M\kappa}} \left(1 + \frac{\tau}{4MD\kappa}\right) \left(\tau\sqrt{\frac{1}{M\kappa}} - \zeta\right) \times \exp\left(-\frac{\tau}{2MD\kappa}\right), \quad (30)$$

$$\rho_b^{(0)}(\zeta, \tau) \simeq \frac{1}{2} + \frac{D}{4}\sqrt{\frac{M}{\kappa}} \left(1 + \frac{\tau MD}{4\kappa}\right) \left(\tau\sqrt{\frac{M}{\kappa}} + \zeta\right) \times \exp\left(-\frac{MD\tau}{2\kappa}\right). \quad (31)$$

Since $\tau \ll \kappa$, the density profiles inside the reaction zone assume a linear behavior in space ζ and time τ as shown below:

$$\rho_a^{(0)}(\zeta, \tau) \simeq \frac{1}{2} + \frac{\tau}{4DM\kappa} - \frac{1}{4D\sqrt{M\kappa}}\zeta, \quad (32)$$

$$\rho_b^{(0)}(\zeta, \tau) \simeq \frac{1}{2} + \frac{MD}{4\kappa}\tau + \frac{1}{4}D\sqrt{\frac{M}{\kappa}}\zeta. \quad (33)$$

Contrary to the parabolic front, the hyperbolic front does not admit a single maximum, but rather a global and one or more local maxima. Thus, we find the second aforementioned definition of the front center to be more convenient:

$$\zeta_f = \frac{\int_{-\infty}^{\infty} \zeta R(\zeta, \tau) d\zeta}{\int_{-\infty}^{\infty} R(\zeta, \tau) d\zeta}. \quad (34)$$

By using Eqs. (32) and (33), we find that the front center scales approximately as a linear function in time as computed from

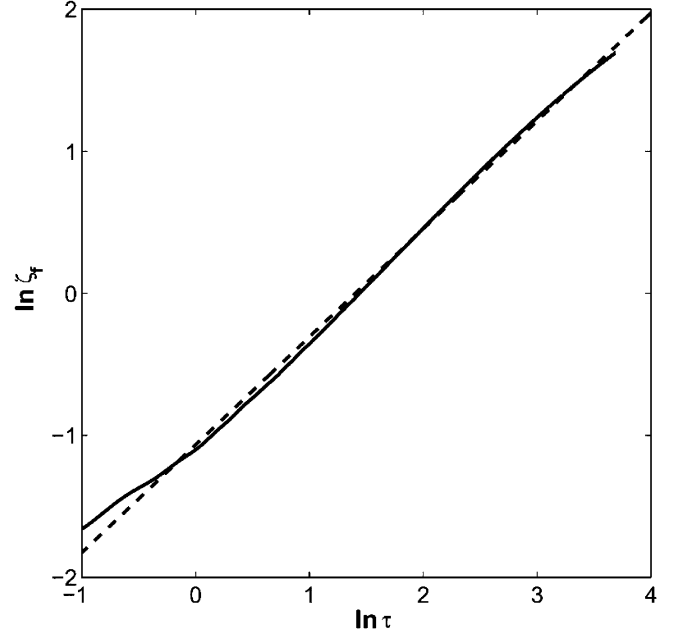


FIG. 1. A plot of the natural logarithm of the hyperbolic reaction center ζ_f as a function of the natural logarithm of time τ . The solid straight line has a slope equal to 0.98, close to 1.0, the slope of the dashed line. This confirms the linear hyperbolic scaling of the front. The parameters used are $\kappa = 5$, $\epsilon = 0.1$, $r = 1$, $D = 2$, $M = 0.5$, and $n = m = 1$.

the full numerical solution of Eqs. (11) and (12) and shown in Fig. 1. Based on this result, we can write the front center in the form $\zeta_f = \tau f(\tau)/g(\tau)$ where

$$f(\tau) = \int_{\zeta^* - \zeta_f}^{\zeta^* + \zeta_f} z \left[\frac{1}{2} + \left(\frac{1}{4DM\kappa} - \frac{1}{4D\sqrt{M\kappa}}z \right) \tau \right]^n \times \left[\frac{1}{2} + \left(\frac{MD}{4\kappa} + \frac{1}{4}D\sqrt{\frac{M}{\kappa}}z \right) \tau \right]^m dz, \quad (35)$$

$$g(\tau) = \int_{\zeta^* - \zeta_f}^{\zeta^* + \zeta_f} \left[\frac{1}{2} + \left(\frac{1}{4DM\kappa} - \frac{1}{4D\sqrt{M\kappa}}z \right) \tau \right]^n \times \left[\frac{1}{2} + \left(\frac{MD}{4\kappa} + \frac{1}{4}D\sqrt{\frac{M}{\kappa}}z \right) \tau \right]^m dz. \quad (36)$$

$z = \zeta/\tau$ and ζ^* is located in the neighborhood of ζ_f . The functions $f(\tau)$ and $g(\tau)$ are dominated by terms of order 1 as $\tau \rightarrow 0$. Hence, we can write

$$\zeta_f \simeq K_1 \tau + O(\tau^2). \quad (37)$$

The velocity of the front is now bounded and can be written as

$$\lim_{\tau \rightarrow 0} v_f = K_1(D, M), \quad (38)$$

where K_1 is a constant that vanishes for $D = n/m$ and $M = m/n$. On the other hand, the width of the front is defined as the square root of the second moment of $R_0(\zeta, \tau)$,

$$w^2(\tau) = \frac{\int_{-\infty}^{\infty} (\zeta - \zeta_f)^2 R_0(\zeta, \tau) d\zeta}{\int_{-\infty}^{\infty} R_0(\zeta, \tau) d\zeta}. \quad (39)$$

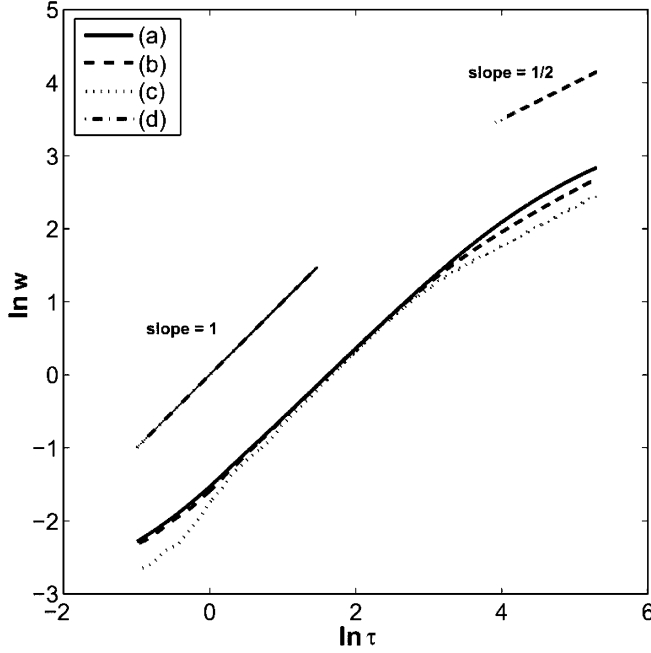


FIG. 2. Plots of the natural logarithm of the width w as a function of the natural logarithm of time τ for different values of n and m . (a) $n = m = 1$; (b) $n = 2, m = 1$; and (c) $n = 3, m = 2$. The width is initially approximately linear in time with the slope equal to 0.94 (a); 0.93 (b); and 0.92 (c). For $\log \tau > 4$ the slope becomes 0.56 (a); 0.55 (b); and 0.53 (c). The straight lines (d) are references with slopes equal to 1 and 1/2. The values of the parameters are $\kappa = 10$, $\epsilon = 0.01$, $r = 1$, $D = 2$, and $M = 0.5$.

The width is computed numerically and in this case leads to a linear scaling in time as shown in Fig. 2.

B. Crossover to the parabolic domain

To keep track of the problem in the parabolic regime, we assume that the hyperbolic equations for this system represent a perturbation of the parabolic equations. At a particular time characteristic of the system, which we denote the crossover time $t_c \sim \sqrt{D_A D_B m_A m_B} / k_b T$, the hyperbolic equation takes a perturbed parabolic form. The numerical solution of Eq. (6) from which we compute the front center ζ_f as a function of time is shown in Fig. 3. This plot clearly exhibits that the front center scales as τ^α with a crossover at $\tau = \tau_c$ from $\alpha \simeq 1$ at early time to $\alpha \simeq 1/2$. Therefore, the hyperbolic regime controls the dynamics of the system until the dimensionless crossover time τ_c is reached, beyond which the system transits to the parabolic regime. From Fig. 4, it is evident that the greater the crossover time the longer the system stays in the hyperbolic regime. In this case, the densities are calculated by taking the limit $\tau/\kappa \rightarrow \infty$ and using the asymptotic expansions (23) and (24) of Eq. (22):

$$\rho_a^{(0)}(\zeta, \tau) \simeq \frac{1}{2} \left[\exp\left(-\frac{\tau}{2MD\kappa}\right) + \operatorname{erf}\left(\frac{1}{2}\sqrt{\frac{\tau}{MD\kappa}}\right) - \operatorname{erf}\left(\frac{1}{2}\sqrt{\frac{\zeta}{\tau D}}\right) \right], \quad (40)$$

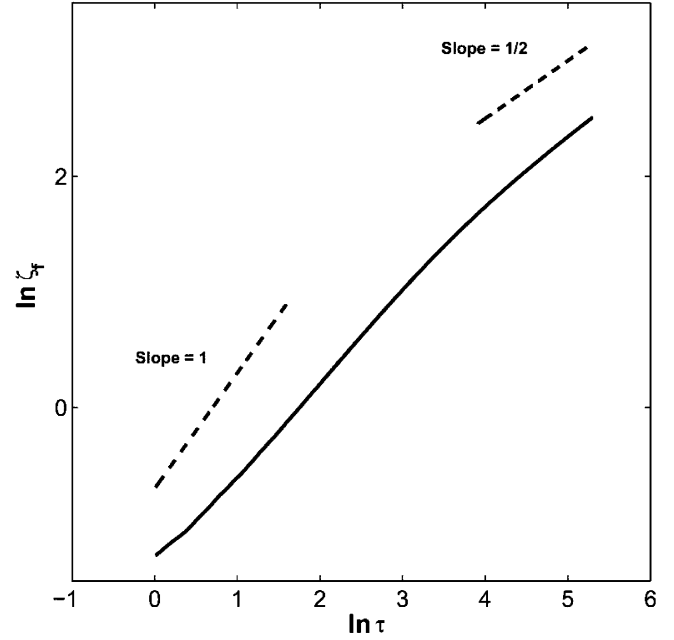


FIG. 3. A plot of the natural logarithm of ζ_f as a function of the natural logarithm of time τ shows the crossover from the hyperbolic (slope $\simeq 1$) to the parabolic regime (slope $\simeq 1/2$). Initially the slope is 0.82, then for $\ln \tau > 4$ the slope is 0.57. Parameters are $\kappa = 10$, $\epsilon = 0.01$, $D = 2$, $M = 0.5$, $n = m = 1$, and $r = 1$.

$$\rho_b^{(0)}(\zeta, \tau) \simeq \frac{1}{2} \left[\exp\left(-\frac{MD\tau}{2\kappa}\right) + \operatorname{erf}\left(\frac{1}{2}\sqrt{\frac{MD\tau}{\kappa}}\right) + \operatorname{erf}\left(\frac{1}{2}\zeta\sqrt{\frac{D}{\tau}}\right) \right]. \quad (41)$$

By doing a Taylor series expansion we find an approximate expression for the local rate

$$R_0(\zeta, \tau) \simeq \frac{1}{2^{m+n}} \left[\operatorname{erf}\left(\frac{1}{2}\sqrt{\frac{\tau}{MD\kappa}}\right) \right]^n \left[\operatorname{erf}\left(\frac{1}{2}\sqrt{\frac{MD\tau}{\kappa}}\right) \right]^m \times [A_1(\tau) - \zeta A_2(\tau) + \zeta^2 A_3(\tau)] \times [B_1(\tau) + \zeta B_2(\tau) + \zeta^2 B_3(\tau)], \quad (42)$$

Eq. (42) is used in the next section to investigate the conditions that should be satisfied to observe a static or moving front. The coefficients A_i and B_i ($i = 1, 2, 3$) depend on time in a complicated manner. Their particular forms are shown in Appendix A 2.

C. The propagating front

The quadratic form of Eq. (42) is taken and then ζ_f is found such that $R_0(\zeta_f) = \max_{\zeta} R_0(\zeta, \tau)$.

$$\zeta_f = \frac{1}{2} \left(\frac{A_1(\tau)B_2(\tau) - A_2(\tau)B_1(\tau)}{A_1(\tau)B_3(\tau) - A_2(\tau)B_2(\tau) + A_3(\tau)B_1(\tau)} \right). \quad (43)$$

For simplicity we take $\exp(-\tau/2MD\kappa) \simeq 0$ with $\tau \gg \kappa$ and introduce the ratio function θ such that $\theta(\tau) = \operatorname{erf}\left(\frac{1}{2}\sqrt{\frac{\tau}{MD\kappa}}\right)/$

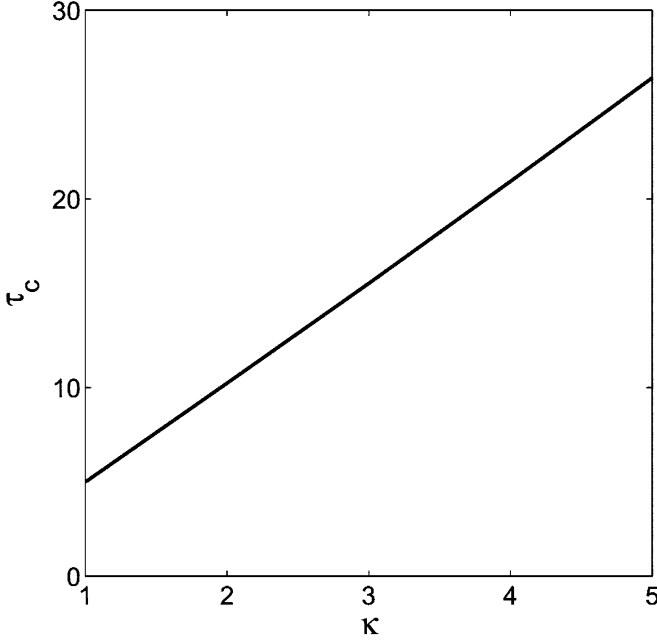


FIG. 4. The crossover time τ_c is a linear function of κ with all other parameters kept constant: $\epsilon = 0.01$, $D = 2$, and $M = 0.5$.

$\text{erf}\left(\frac{1}{2}\sqrt{\frac{MD\tau}{\kappa}}\right)$. The expression for the front becomes

$$\zeta_f = \frac{1}{2}\sqrt{\tau} \left(\frac{\frac{n}{\sqrt{\pi D}} - \sqrt{D}\frac{m}{\sqrt{\pi}}\theta}{\frac{Dm(m-1)}{2\pi}\theta - \frac{nm}{\pi} + \frac{n(n-1)}{2D\pi}\frac{1}{\theta}} \right) \text{erf}\left(\frac{1}{2}\sqrt{\frac{MD\tau}{\kappa}}\right). \quad (44)$$

For the particular case of equal reactant time scales, that is, $MD = 1$, θ is unity which reduces Eq. (44) to the simpler form

$$\zeta_f = \zeta_f^p \left[1 - \text{erfc}\left(\frac{1}{2}\sqrt{\frac{\tau}{\kappa}}\right) \right], \quad (45)$$

where ζ_f^p is the parabolic front center

$$\zeta_f^p = -\sqrt{\pi} \left(\frac{\sqrt{D}m - \frac{n}{\sqrt{D}}}{Dm(m-1) - 2nm + \frac{n(n-1)}{D}} \right) \tau^{1/2}, \quad (46)$$

Eq. (45) can be thought of as a perturbed form of Eq. (46). We note that irrespective of the direction the front moves in, the correction function $\zeta_f^p \text{erfc}\left(\frac{1}{2}\sqrt{\frac{\tau}{\kappa}}\right)$ acts in the opposite sense by reducing the magnitude of ζ_f . This is precisely what the hyperbolic equation is expected to do, to slow down the speed of the propagating front. Equation (46) can be reduced to the result derived in [3] by setting $n = m = 1$.

D. The static front

The front is static when ζ_f vanishes. Therefore, from Eq. (44) it is obvious that the following conditions must be met:

$$D = n/m, \quad (47)$$

$$M = m/n. \quad (48)$$

Table I summarizes the conditions necessary to observe a static or moving front. In Figs. 5 and 6 the conditions for a static front

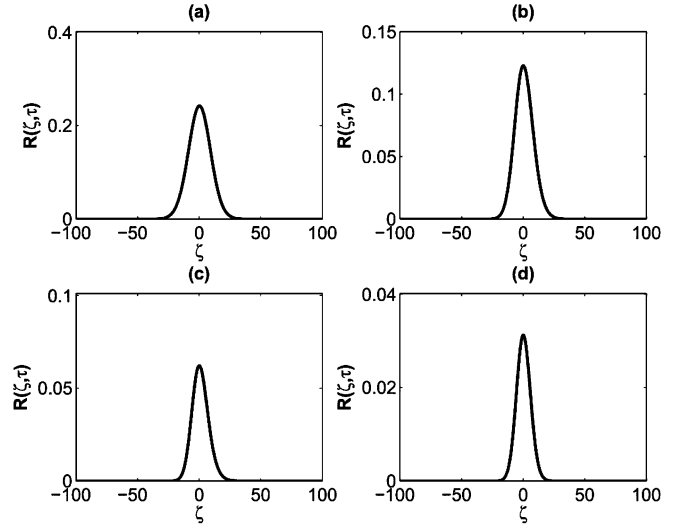


FIG. 5. The parabolic system with a static front at $\tau = 50$, $D = n/m$, $\epsilon = 10^{-3}$, and $r = 0.5$ for different stoichiometries: (a) $A + B \rightarrow C$; (b) $2A + B \rightarrow C$; (c) $3A + B \rightarrow C$; and (d) $3A + 2B \rightarrow C$.

are investigated numerically and are confirmed for both the parabolic Eqs. (17) and (18) and hyperbolic systems Eqs. (11) and (12) with different chemical reactions.

E. Width scaling

We have shown numerically that the width scales as a linear function of time when the hyperbolic regime dominates. In the parabolic and short-time limit, the width of the front scales in time as $w \sim \tau^{1/2}$ independent of the stoichiometric

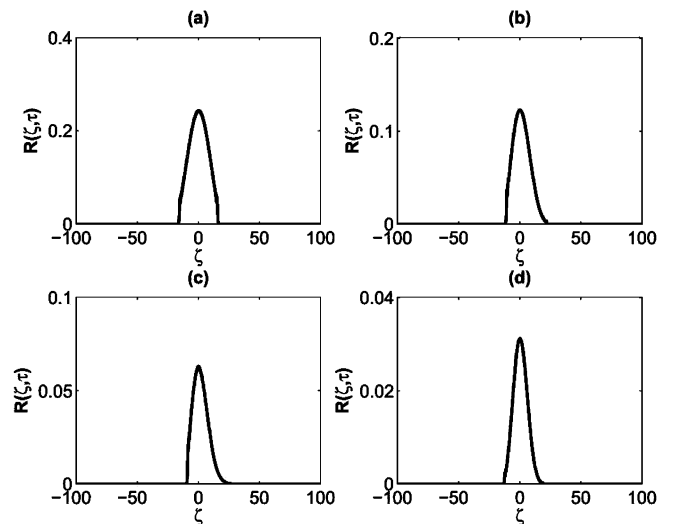


FIG. 6. The hyperbolic system with a static front at $\tau = 50$, $\kappa = 10$, $\epsilon = 10^{-3}$, $D = n/m$, $M = m/n$, and $r = 0.5$ for different stoichiometries: (a) $A + B \rightarrow C$; (b) $2A + B \rightarrow C$; (c) $3A + B \rightarrow C$; and (d) $3A + 2B \rightarrow C$.

TABLE I. Conditions for static or moving fronts for different reaction stoichiometries.

Stoichiometry	$n = m$		$n \neq m$	
	$D = 1, M = 1$	$D \neq 1$ or $M \neq 1$	$D = n/m$ and $M = m/n$	$D \neq n/m$ or $M \neq m/n$
Condition	Static	Moving	Static	Moving
Front Dynamics	Static	Moving	Static	Moving

coefficients, unlike its asymptotic behavior [9,34]. Let $q = \zeta/\sqrt{\tau}$, then Eq. (27) can be recast in the form

$$R_0(q, \tau) \simeq \frac{1}{2^{n+m}} \left[\operatorname{erf} \left(\frac{1}{2} \sqrt{\frac{\tau}{MD\kappa}} \right) \right]^n \left[\operatorname{erf} \left(\frac{1}{2} \sqrt{\frac{MD\tau}{\kappa}} \right) \right]^m \times \Lambda(q, \tau), \quad (49)$$

where

$$\Lambda(q, \tau) = \left[1 - \frac{\operatorname{erf} \left(\frac{1}{2} \frac{q}{\sqrt{D}} \right)}{\operatorname{erf} \left(\frac{1}{2} \sqrt{\frac{\tau}{MD\kappa}} \right)} \right]^n \left[1 + \frac{\operatorname{erf} \left(\frac{1}{2} q \sqrt{D} \right)}{\operatorname{erf} \left(\frac{1}{2} \sqrt{\frac{MD\tau}{\kappa}} \right)} \right]^m. \quad (50)$$

The expression for the width from Eq. (39) becomes

$$w^2(\tau) \simeq \tau \times I_w(\tau), \quad (51)$$

where

$$I_w(\tau) = \frac{\int_{-\infty}^{\infty} q^2 \Lambda(q, \tau) dq}{\int_{-\infty}^{\infty} \Lambda(q, \tau) dq}. \quad (52)$$

Although in general we cannot evaluate the integral I_w , we expect it to converge to a constant value independent of time. For $n = m = 1$, it can be solved exactly, and for the general case we can evaluate the integral by taking a binomial expansion of the integrand, which is based on the assumption that the main contribution of the integral lies within the neighborhood of ζ_f . (see Appendix A 3).

$$I_w \simeq 2 \left(\frac{2D^4 + D^2 + 2}{3D(D^2 + 1)} \right). \quad (53)$$

Since the width approaches the scaling $w \sim \tau^{1/2}$ as $\kappa/\tau \rightarrow 0$, initially the stoichiometry plays no role in the scaling of the parabolic width. To confirm this result, we solve numerically Eq. (6) for chemical reactions with various stoichiometries, compute the width using Eq. (39), and compare it with the approximate form in Eq. (51) for the width. This comparison is shown in Fig. 7, where we confirm that the log-log plot of w versus τ is linear with its slope close to $1/2$.

F. Global rate scaling

Following Gálfi and Rácz [1], the global rate $\mathfrak{R}_0(\tau)$ is defined as

$$\mathfrak{R}_0(\tau) = \int_{-\infty}^{\infty} R_0(\zeta, \tau) d\zeta, \quad (54)$$

which can be explicitly written as

$$\mathfrak{R}_0(\tau) \simeq \left[\operatorname{erf} \left(\frac{1}{2} \sqrt{\frac{\tau}{MD\kappa}} \right) \right]^n \left[\operatorname{erf} \left(\frac{1}{2} \sqrt{\frac{MD\tau}{\kappa}} \right) \right]^m \tau^{1/2} I_R, \quad (55)$$

where

$$I_R(\tau) = \frac{1}{2^{n+m}} \int_{-\infty}^{\infty} \Lambda(q, \tau) dq. \quad (56)$$

We expect the integral I_R to approach a constant as $\tau/\kappa \rightarrow \infty$. For $n = m = 1$, this integral can be evaluated exactly, where as for the general case we use the previous approximation that the

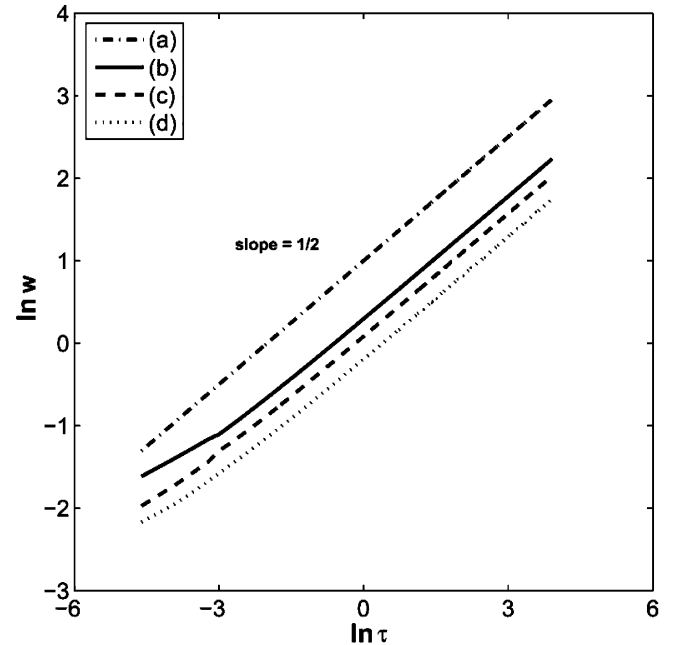


FIG. 7. Plots for the natural logarithm of the width w as a function of the natural logarithm of time τ with $D = 1.5$, $\epsilon = 10^{-3}$, and $r = 0.5$ for different stoichiometries: (b) $n = m = 1$, slope = 0.493; (c) $n = 2$, $m = 1$, slope = 0.495; and (d) $n = 3$, $m = 2$, slope = 0.498. The reference line (a) has a slope equal to $1/2$.

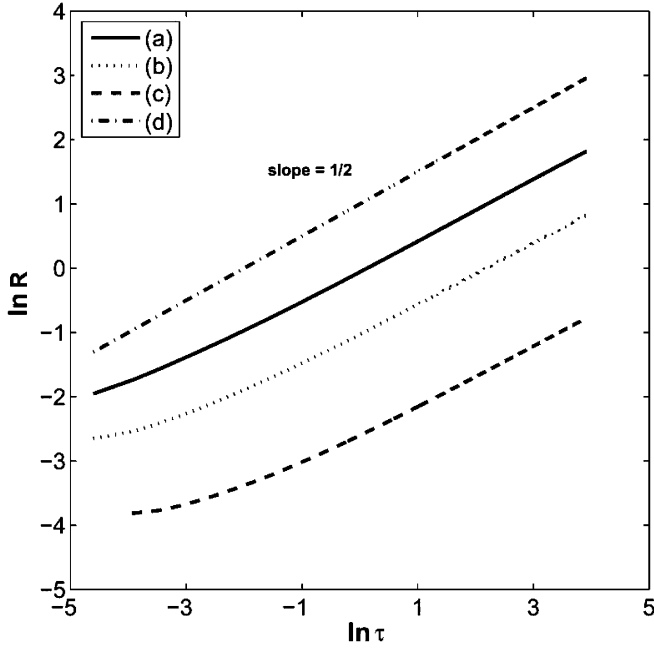


FIG. 8. Plots of the natural logarithm of the global rate R as a function of the natural logarithm of time τ with $\epsilon = 10^{-3}$, $r = 1$, and $D = 2$ for different stoichiometries: (b) $n = m = 1$, slope = 0.48; (c) $n = 2, m = 1$, slope = 0.47; and (d) $n = 3, m = 2$, slope = 0.46. The reference line (a) has a slope equal to $1/2$.

main contribution to the integral lies within the neighborhood of ζ_f .

$$I_R(\tau) \simeq \frac{nm}{2^{n+m-2}\sqrt{\pi}} \left[\operatorname{erf} \left(\frac{1}{2} \sqrt{\frac{\tau}{MD\kappa}} \right) \times \operatorname{erf} \left(\frac{1}{2} \sqrt{\frac{MD\tau}{\kappa}} \right) \right]^{-1} \sqrt{D + \frac{1}{D}}. \quad (57)$$

The global rate approaches the parabolic limit scaling $\mathfrak{R}_0(\tau) \sim \tau^{1/2}$ as $\kappa/\tau \rightarrow 0$. The numerical solution for the global rate is shown in Fig. 8 and confirms this result for different stoichiometries.

IV. FIRST ORDER SOLUTION: INTERMEDIATE TIME BEHAVIOR

In order to investigate the scaling laws near the region where the chemical reaction begins to play a significant role, we shall find the solution to the first order terms in ϵ in the perturbation expansion of Eqs. (11) and (12). As we discussed earlier, when we exit the hyperbolic regime after the crossover time τ_c , the chemical reaction dominates over diffusion, and we can neglect any hyperbolic corrections to the resulting equations. This in turn gives rise to the following first order equations:

$$\partial_\tau \rho_a^{(1)} = D \Delta_\zeta \rho_a^{(1)} - nr R_0, \quad (58)$$

$$\partial_\tau \rho_b^{(1)} = D^{-1} \Delta_\zeta \rho_b^{(1)} - \frac{m}{r} R_0. \quad (59)$$

The solution to the inhomogeneous diffusion equation can be expressed using Green's function as

$$\rho_a^{(1)}(\zeta, \tau) = -\frac{rn}{2\sqrt{\pi D}} \int_0^\tau \int_{-\infty}^\infty \frac{1}{\sqrt{\tau-k}} \left[1 - \operatorname{erf} \left(\frac{\xi}{2\sqrt{Dk}} \right) \right]^n \times \left[1 + \operatorname{erf} \left(\frac{\xi\sqrt{D}}{2\sqrt{k}} \right) \right]^m \exp \left[-\frac{(\xi-x)^2}{4D(\tau-k)} \right] d\xi dk. \quad (60)$$

The solution for $\rho_b^{(1)}$ is the same as for $\rho_a^{(1)}$ in Eq. (60) except we replace D by D^{-1} and nr by m/r . The integrals in Eq. (60) can be fitted to Gaussian-like functions to yield the following first order solutions:

$$\rho_a^{(1)}(\zeta, \tau) = -\frac{rn}{2\sqrt{\pi D}} \tau \exp \left\{ -\frac{1}{4} \left[\frac{\zeta}{\sqrt{D\tau}} - \left(\frac{n}{\sqrt{D}} - m\sqrt{D} \right) \right]^2 - \frac{1}{4D} \right\}, \quad (61)$$

$$\rho_b^{(1)}(\zeta, \tau) = -\frac{m\sqrt{D}}{2r\sqrt{\pi}} \tau \exp \left\{ -\frac{1}{4} \left[\frac{\zeta}{\sqrt{\tau}} \sqrt{D} - \left(\frac{n}{\sqrt{D}} - m\sqrt{D} \right) \right]^2 - \frac{D}{4} \right\}. \quad (62)$$

Equations (61) and (62) are checked numerically and found to be well validated. For $n = m = 1$, the results published in [23] are recovered. The local rate expression can be found by using the following expansion:

$$R(\zeta, \tau) = R_0(\zeta, \tau) + \epsilon R_1(\zeta, \tau) + O(\epsilon^2), \quad (63)$$

where

$$R_1 = n\rho_a^{(1)}(\rho_a^{(0)})^{n-1}(\rho_b^{(0)})^m + m\rho_b^{(1)}(\rho_a^{(0)})^n(\rho_b^{(0)})^{m-1}. \quad (64)$$

We can determine the expression for the center of the front ζ_f from the maximum of the quadratic form of the rate, and it is found to be

$$\zeta_f = \frac{\frac{1}{\sqrt{\pi\tau}}(m\sqrt{D} - \frac{n}{\sqrt{D}}) + \epsilon N_1(D, r)\sqrt{\tau}}{\frac{1}{\pi\tau}(-\frac{n^2}{D} + mD - m^2D + \frac{n}{D} + 2mn) + \epsilon N_2(D, r)}. \quad (65)$$

The front is now static when not only $D = n/m$ but also, when $N_1(D, r) = 0$. It can be shown that at $r = \sqrt{\exp(\frac{1}{4D} - \frac{D}{4})}$, N_1 vanishes. Therefore, in total the three equations that must hold true for the front to be static are

$$M = m/n, \quad (66)$$

$$D = n/m, \quad (67)$$

$$r = \sqrt{\exp \left(\frac{1}{4D} - \frac{D}{4} \right)}. \quad (68)$$

We note that for the parabolic equation only the second and third conditions must be satisfied. Furthermore, by taking the case $n = m$, we immediately recover the conditions for a static front derived in [3], namely, $D = 1$ and $r = 1$. The

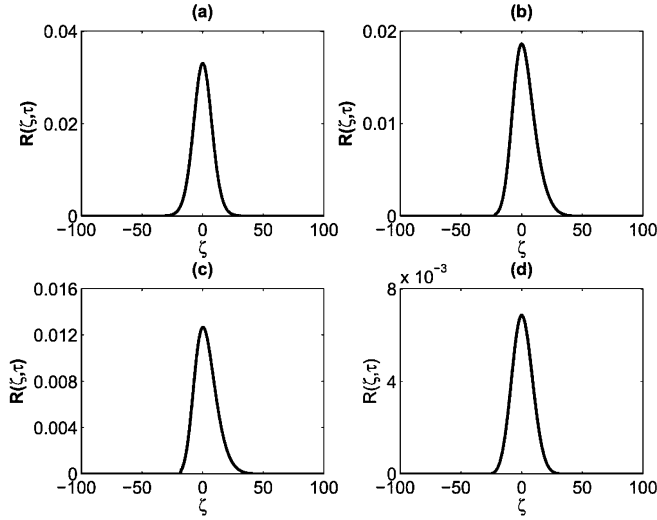


FIG. 9. A static parabolic front center at $\tau = 100$ with $D = n/m$, $r = \sqrt{\exp(\frac{1}{4D} - \frac{D}{4})}$, and $\epsilon = 0.1$ for different stoichiometries: (a) $A + B \rightarrow$; (b) $2A + B \rightarrow C$; (c) $3A + B \rightarrow C$; and (d) $3A + 2B \rightarrow C$.

numerical simulations shown in Fig. 9 confirm the validity of the derived conditions in Eqs. (66)–(68). For $D = n/m$ and $r \neq \sqrt{\exp(\frac{1}{4D} - \frac{D}{4})}$, the front center equation becomes

$$\zeta_f = \frac{\epsilon N_1(r) \tau^{3/2}}{\frac{1}{\pi}(n+m) + \epsilon \tau N_2(r)}. \quad (69)$$

For $\epsilon \ll 1$ the front scales as $\zeta_f \sim \tau^{3/2}$. The numerical solution confirms this scaling result as shown in Fig. 10, where the slopes of the log-log plot are close to 3/2 for various

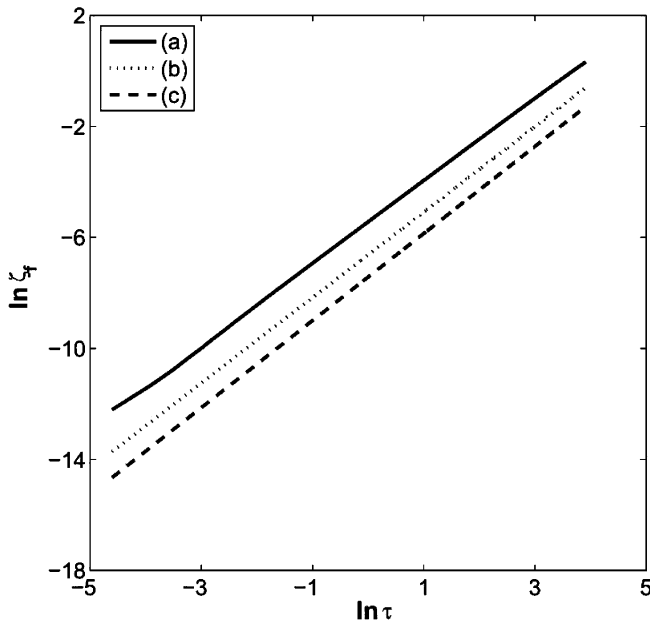


FIG. 10. Plots of the natural logarithm of the front center ζ_f as a function of the natural logarithm of time τ with $D = n/m$, $r = 0.5$, and $\epsilon = 10^{-2}$ for different stoichiometries: (a) $n = m = 1$; (b) $n = 2, m = 1$; and (c) $n = 3, m = 2$. The slope is 1.44 (a); 1.54 (b); and 1.56 (c).

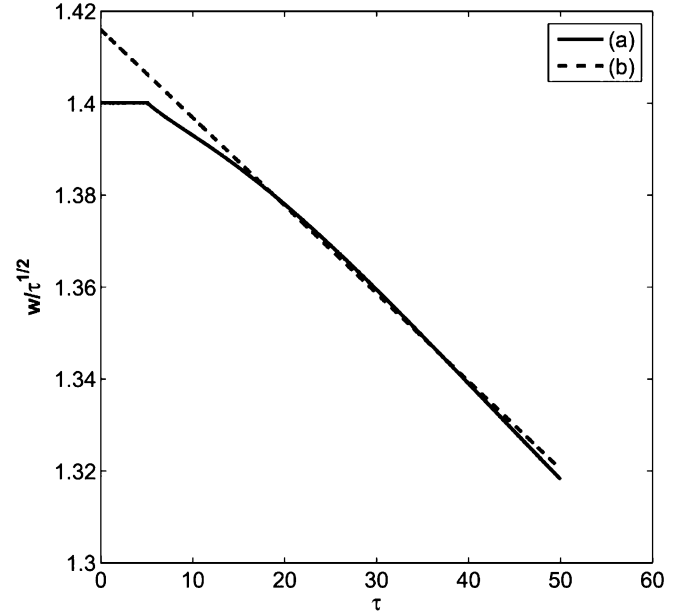


FIG. 11. A plot of $w/\tau^{1/2}$ as a function of τ for $n = m = 1$, $D = 2$, $r = 0.1$, and $\epsilon = 10^{-2}$. The slope of line (a) is equal to 0.98, close to 1.0 (b). This suggests that the width crosses over from $\tau^{1/2}$ to $\tau^{3/2}$ at intermediate times. For reasons of numerical stability, the width is initially computed symbolically and exhibits fluctuations around an average value of 1.4.

stoichiometries. In order to see how the width scales in time, we shall find its temporal evolution up to first order correction with ϵ being quite small and $\zeta_f \sim \sqrt{\tau}$. The expression for the width becomes:

$$w^2(\tau) \simeq \tau K_{w,1} + \epsilon K_{w,2} \tau^2, \quad (70)$$

where $K_{w,1}$ and $K_{w,2}$ are constants. A Taylor series expansion of the square root of Eq. (70) leads to the approximation for the width shown in the following,

$$w(\tau) \simeq w_0(\tau) \{1 + K_w \epsilon \tau\} + O(\epsilon^2), \quad (71)$$

where we previously determined that $w_0(\tau) \sim \tau^{1/2}$ and $K_w = K_{w,2}/2K_{w,1}$. The second scaling term is thus proportional to $\tau^{3/2}$. In order to confirm this scaling, we plot $w/\tau^{1/2}$ as a function of τ and obtain a straight line with a negative slope as shown in Fig. 11. In the asymptotic limit the width crosses over with a scaling in time of the form $\tau^{(1/2)-\sigma}$ with $\sigma = 1/(n+m+1)$ [9,34].

V. NUMERICAL METHOD

The method of lines is employed to solve Eq. (6) on a one-dimensional grid. The cell-centered finite volume scheme is used for the spatial discretization. The finite volume method is widely employed for conservative partial differential equations. We assume that the system admits a unique solution in the region of space Ω bounded by $\partial\Omega$ at any time τ . At the boundaries, the Dirichlet boundary conditions are imposed:

$$\rho_a(\infty, \tau) = 0, \quad \rho_b(\infty, \tau) = 1, \quad (72)$$

$$\rho_a(-\infty, \tau) = 1, \quad \rho_b(-\infty, \tau) = 0. \quad (73)$$

The initial conditions are specified through the Heaviside unit step function:

$$\rho_a(\zeta, 0) = H(-\zeta), \quad \partial_t \rho_a(\zeta, 0) = 0, \quad (74)$$

$$\rho_b(\zeta, 0) = H(\zeta), \quad \partial_t \rho_b(\zeta, 0) = 0. \quad (75)$$

We begin by integrating the equations over the whole domain

$$\begin{aligned} \int_{\Omega} \partial_{\tau} \rho_a dV &= D \int_{\Omega} \nabla \cdot \nabla_{\zeta} \rho_a dV - c\kappa \int_{\Omega} \partial_{\tau\tau}^2 \rho_a dV \\ &\quad - nr\epsilon \int_{\Omega} \rho_a^n \rho_b^m dV - ncr\epsilon\kappa \int_{\Omega} \partial_{\tau} (\rho_a^n \rho_b^m) dV, \end{aligned} \quad (76)$$

$$\begin{aligned} \int_{\Omega} \partial_{\tau} \rho_b dV &= \frac{1}{D} \int_{\Omega} \nabla \cdot \nabla_{\zeta} \rho_b dV - \frac{1}{c} \kappa \int_{\Omega} \partial_{\tau\tau}^2 \rho_b dV \\ &\quad - \frac{m}{r} \epsilon \int_{\Omega} \rho_a^n \rho_b^m dV - \frac{m}{cr} \epsilon \kappa \int_{\Omega} \partial_{\tau} (\rho_a^n \rho_b^m) dV. \end{aligned} \quad (77)$$

The parameter c is equal to MD . The domain Ω is partitioned into a finite number of control volumes, each of which is a rectangle of height one. Across each we apply a first order Gauss quadrature (at the centroid of each control volume) to numerically integrate the equations. Using the divergence theorem we get

$$\begin{aligned} \partial_{\tau} \rho_a &= \frac{D}{V} \oint_{\partial\Omega} \nabla_{\zeta} \rho_a \cdot \mathbf{n} d\mathcal{L} - c\kappa \partial_{\tau\tau}^2 \rho_a - nr\epsilon \rho_a^n \rho_b^m \\ &\quad - ncr\epsilon\kappa \partial_{\tau} (\rho_a^n \rho_b^m), \end{aligned} \quad (78)$$

$$\begin{aligned} \partial_{\tau} \rho_b &= \frac{1}{DV} \oint_{\partial\Omega} \nabla_{\zeta} \rho_b \cdot \mathbf{n} d\mathcal{L} - \frac{1}{c} \kappa \partial_{\tau\tau}^2 \rho_b - \frac{m}{r} \epsilon \rho_a^n \rho_b^m \\ &\quad - \frac{m}{cr} \epsilon \kappa \partial_{\tau} (\rho_a^n \rho_b^m). \end{aligned} \quad (79)$$

Since diffusion is isotropic, we use the forward difference formula to compute the flux across each face. Define the Laplace operator $\mathbf{L} \in \mathbb{R}^{N_c, N_c}$ and $\mathbf{a}, \mathbf{b} \in \mathbb{R}^{N_c}$, where N_c is the number of control volumes. The system of ordinary differential equations (ODEs) to integrate is written as

$$\begin{aligned} d_{\tau} \mathbf{a} &= D\mathbf{L}\mathbf{a} - c\kappa d_{\tau\tau}^2 \mathbf{a} - nr\epsilon \mathbf{D}_a^{n-1} \mathbf{D}_b^m \mathbf{a} \\ &\quad - ncr\epsilon\kappa d_{\tau} (\mathbf{D}_a^{n-1} \mathbf{D}_b^m \mathbf{a}), \end{aligned} \quad (80)$$

$$\begin{aligned} d_{\tau} \mathbf{b} &= \frac{1}{D} \mathbf{L}\mathbf{b} - \frac{1}{c} \kappa d_{\tau\tau}^2 \mathbf{b} - \frac{m}{r} \epsilon \mathbf{D}_a^n \mathbf{D}_b^{m-1} \mathbf{b} \\ &\quad - \frac{m}{cr} \epsilon \kappa d_{\tau} (\mathbf{D}_a^n \mathbf{D}_b^{m-1} \mathbf{b}), \end{aligned} \quad (81)$$

where d_{τ} is the ordinary time derivative $d/d\tau$, $\mathbf{D}_a = \text{diag}(\mathbf{a})$, and $\mathbf{D}_b = \text{diag}(\mathbf{b})$. To integrate these equations we use the technique of reduction of order to transform the system of second order ODE's to first order, i.e., we solve for $\mathbf{u} = d_{\tau} \mathbf{a}$ and $\mathbf{v} = d_{\tau} \mathbf{b}$. We use variable order backward differentiation formulas (BDFs) to integrate the equations with an adaptive scheme where the time step taken is computed in such a way that the absolute error is less than 10^{-3} . Such a scheme is highly suitable for stiff differential equations. In order to make the computations faster and avoid solving for a $2N_c \times 2N_c$ reduced Jacobian, we split the four equations into two systems (for each we solve once for an $N_c \times N_c$ matrix) and linearize them by invoking a fixed-point iteration scheme,

the convergence of which is usually linear and not quadratic as in Newton's method. However, since the system does not have very stiff source terms, convergence is very rapid (two to three iterations per time step). Thus, the order of convergence is relatively less important than the size of the operator. For the A component, the linearized system is

$$\begin{pmatrix} \mathbf{D}_{11} & \mathbf{D}_{12} \\ \lambda_0 \mathbf{I} & -\mathbf{I} \end{pmatrix}_{j-1} \begin{pmatrix} \mathbf{a}^k \\ \mathbf{u}^k \end{pmatrix}_j = \begin{pmatrix} c\kappa \sum_{i=1}^N \lambda_i \mathbf{u}^{k-i} \\ \sum_{i=1}^N \lambda_i \mathbf{a}^{k-i} \end{pmatrix}, \quad (82)$$

where

$$\begin{aligned} \mathbf{D}_{11} &= nr\epsilon (\mathbf{D}_a^k)^{n-1} (\mathbf{D}_b^k)^m \\ &\quad + nmc\kappa r\epsilon \kappa (\mathbf{D}_a^k)^{n-1} (\mathbf{D}_b^k)^{m-1} \mathbf{D}_v^k - D\mathbf{L}, \end{aligned} \quad (83)$$

$$\mathbf{D}_{12} = (1 + c\kappa\lambda_0)\mathbf{I} + n^2 c\kappa r\epsilon \kappa (\mathbf{D}_a^k)^{n-1} (\mathbf{D}_b^k)^m, \quad (84)$$

where $\{\lambda_i, i \leq N\}$ is the set of BDF coefficients with N being the order of the BDF used, \mathbf{I} is the identity matrix, $\mathbf{D}_v = \text{diag}(\mathbf{v})$, j signifies the current iteration number, and k is the current time step taken. Equation (82) can be rearranged to yield the recursive system of equations

$$\begin{aligned} &[(\mathbf{D}_{11})_{j-1} + \lambda_0 (\mathbf{D}_{12})_{j-1}] \mathbf{a}_j^k \\ &= c\kappa \sum_{i=1}^N \lambda_i \mathbf{u}^{k-i} + (\mathbf{D}_{12})_{j-1} \sum_{i=1}^N \lambda_i \mathbf{a}^{k-i}, \end{aligned} \quad (85)$$

$$\mathbf{u}_j^k = \lambda_0 \mathbf{a}_j^k - \sum_{i=1}^N \lambda_i \mathbf{a}^{k-i}. \quad (86)$$

Equation (85) can be solved efficiently with the Thomas algorithm for tridiagonal matrices. A similar set of equations can be easily constructed for the B component. The two systems are solved simultaneously until convergence with a tolerance of 10^{-6} .

VI. COMPARISON TO MOLECULAR DYNAMICS AND EXPERIMENTAL OUTLOOK

The newly derived scaling laws were compared to those derived from recent simulation studies on non-Fickian diffusion which are usually centered in the area of mass transport in polymers. Yaneva *et al.* [48] used dissipative particle molecular dynamics to study a model of a binary mixture of two species with different diffusion coefficients and obtained a non-Fickian behavior in the case of strongly asymmetric systems ($D_A \gg D_B$). This system significantly resembled the physics we studied in this paper. The noticeable similarities between the simulations and our results were that a linear dependence of the position of the front ($x_f \sim t$) was observed indicating anomalous diffusion which crossed over to the Fickian regime ($x_f \sim t^{1/2}$) after some time. Furthermore, according to the simulation results, this deviation from Fickian diffusion was independent from molecular details and requires only two conditions to be reached: a sizable difference in mobilities of the two species and a so-called plasticizing

effect whereby the slow species acquire a higher mobility when surrounded by the fast species, for example, due to a chemical reaction or a dissolution process of the underlying matrix. It was also argued that recent molecular dynamics and grand canonical Monte Carlo simulations by Tsige and Grest [49] failed to predict the anomalous diffusion, possibly due to an underrepresentation of the plasticizing effect in their simulations.

Those simulation results gave new insight to the experimental verification of the new scaling law during the short-time regime. The ongoing experiments are based on the diffusion of sulfide ions into a gelatin matrix containing cadmium ions and a capping agent to slow down the growth of the reaction product. The cadmium ions are confined to the matrix due to the binding of gelatin to those ions, making a considerable difference between the mobilities of the invading sulfide ions and the residing cadmium ions. Moreover, the plasticizing effect is strongly present in this system because of the liberation of the cadmium ions from gelatin in the vicinity of the reaction zone. When the concentration of those ions is small, the reaction between them yields a propagating front of fluorescent cadmium sulfide quantum dots. By using fluorescence techniques, we were able to follow the front and analyze its concentration changes during evolution [50]. We are now in the process of exploring the parameter space and seek anomalous diffusion of the reaction front.

VII. CONCLUSION

In this paper, we present a model for front propagation of initially separated components using hyperbolic reaction-diffusion equations. Contrary to their parabolic counterpart, the hyperbolic equations yield a finite speed of propagation, rendering them more suitable to study this kind of problem. We show that asymptotically, for smooth initial data, the hyperbolic equations yield the parabolic equations, hence the asymptotic scaling laws are the same. However, using perturbation techniques, we show that scaling laws for the reaction center, the width, and reaction rate for the short-time regime are quite different and appear to be independent of the stoichiometric coefficients of the reactants. While the short-time behavior scales as $\tau^{1/2}$ for the reaction center, width, and global reaction rate in the case of the parabolic system, it scales linearly in time for the hyperbolic counterpart. Criteria for the moving and static front are also derived and compared with those derived for the parabolic case. The posthyperbolic regime was also investigated using first order perturbation solution. The perturbation results are compared with full numerical integration of the hyperbolic equations. There are also some interesting peculiarities found in the numerical solutions of the hyperbolic equations at early times, not found for the solutions of the parabolic equations, such as wave splitting and recombination, that are worth further investigation. In addition, other chemical kinetic models, such as those involving autocatalysis such as $A + B \rightarrow 2A$, are also currently under consideration. The aim is to investigate front velocity selection in such systems using the hyperbolic version of the reaction-diffusion equations and compare them to the interesting Monte Carlo results

by Mai *et al.* [31] that delineated resolutely the role of fluctuations in velocity selection. We are also making use of the semianalytic results of this paper to understand revert spacing in some Liesegang systems. We refer the reader to future papers.

ACKNOWLEDGMENTS

The authors would like to acknowledge the support of grants from the Lebanese Council for Scientific Research (LCNSR) and from the University Research Board, American University of Beirut.

APPENDIX

1. Asymptotic behavior of the hyperbolic diffusion equation

Consider the map $f: \mathbb{R}^{n+1} \rightarrow \mathbb{R}$, where the image f is defined through the hyperbolic differential equation

$$\partial_\tau f = \Delta f + \kappa \partial_{\tau\tau} f, \quad (\text{A1})$$

where Δ is the Laplacian, $f(\mathbf{u}, \tau) \in \mathbb{C}^2$, $\mathbf{u} \in \mathbb{R}^n$, $\kappa \in \mathbb{R}^*$, and n is the spatial dimension number. Define the transformation $(\mathbf{u}, \tau) \rightarrow (\eta, \sigma)$ such that

$$\eta = \tau^{-\alpha} \sum_{i=1}^n u_i, \quad (\text{A2})$$

$$\sigma = \ln \tau^\beta, \quad (\text{A3})$$

where $\alpha \in \mathbb{R}^*$ and $\beta \geq 1$. Direct application of the chain rule leads to the following equations:

$$\partial_\tau = \beta e^{-\sigma/\beta} \partial_\sigma - \alpha \eta e^{-\sigma/\beta} \partial_\eta, \quad (\text{A4})$$

$$\partial_{\tau\tau}^2 = e^{-2\sigma/\beta} [\beta^2 \partial_{\sigma\sigma}^2 - \beta \partial_\sigma - 2\alpha \beta \eta \partial_{\sigma\eta}^2 + \alpha(\alpha + 1) \eta \partial_\eta + \alpha^2 \eta^2 \partial_{\eta\eta}^2], \quad (\text{A5})$$

$$\Delta = n e^{-(2\alpha/\beta)\sigma} \partial_{\eta\eta}^2. \quad (\text{A6})$$

In the newly defined coordinate system Eq. (A1) becomes

$$\beta \partial_\sigma f - \alpha \eta \partial_\eta f = n e^{(1-2\alpha)\sigma/\beta} \partial_{\eta\eta}^2 f + \kappa e^{-\sigma/\beta} [\beta^2 \partial_{\sigma\sigma}^2 - \beta \partial_\sigma - 2\alpha \beta \eta \partial_{\sigma\eta}^2 + \alpha(\alpha + 1) \eta \partial_\eta + \alpha^2 \eta^2 \partial_{\eta\eta}^2] f. \quad (\text{A7})$$

Without loss of generality let $\alpha = \frac{1}{2}$, then

$$\beta \partial_\sigma f - \frac{1}{2} \eta \partial_\eta f = n \partial_{\eta\eta}^2 f + \kappa e^{-\sigma/\beta} [\beta^2 \partial_{\sigma\sigma}^2 - \beta \partial_\sigma - \beta \eta \partial_{\sigma\eta}^2 + \frac{3}{4} \eta \partial_\eta + \frac{1}{4} \eta^2 \partial_{\eta\eta}^2] f. \quad (\text{A8})$$

By performing a similarity transformation by taking $\eta = G(\sigma)$ and introducing the inverse relation $\sigma = \Theta(\eta)$, we can show that

$$\begin{aligned} & n d_{\eta\eta}^2 f + \frac{1}{2} \eta d_\eta f \\ & = \beta \Theta_\eta^{-1} d_\eta f - \kappa e^{-\Theta/\beta} [\beta^2 \Theta_\eta^{-1} d_\eta \Theta_\eta^{-1} d_\eta - \beta \Theta_\eta^{-1} d_\eta \\ & \quad - \beta \eta \Theta_\eta^{-1} d_{\eta\eta}^2 + \frac{3}{4} \eta d_\eta + \frac{1}{4} \eta^2 d_{\eta\eta}^2] f. \end{aligned} \quad (\text{A9})$$

We have used the notation $\Theta_\eta = d_\eta \Theta$. It is easy to prove that $\Theta(\eta) = \frac{\beta}{\alpha} \ln(\sum_{i=1}^n \mathbf{u}_i / \eta)$, then as $\tau \rightarrow \infty$, $\Theta(\eta) \rightarrow \infty$ and $\Theta_\eta(\eta) \rightarrow -\infty$. Taking this into account for Eq. (A9), it becomes apparent that

$$\lim_{\tau \rightarrow \infty} n d_{\eta\eta}^2 f + (2)^{-1} \eta d_\eta f = 0. \quad (\text{A10})$$

For $n = 1$, we recover the following ordinary differential form of the parabolic diffusion equation in one dimension

$$\lim_{\tau \rightarrow \infty} d_{\eta\eta}^2 f + \frac{1}{2} \eta d_\eta f = 0. \quad (\text{A11})$$

The parabolic equation is readily obtained once a reverse similarity transformation is done on Eqs. (A2) and (A3) to give

$$\begin{aligned} d_\eta &= -2 \frac{\tau}{\eta} \partial_\tau, \\ d_{\eta\eta}^2 &= \tau \partial_{u_1 u_1}^2, \end{aligned} \quad (\text{A12})$$

which in turn leads to the partial differential equation

$$\tau (\partial_{u_1 u_1}^2 - \partial_\tau) f = 0. \quad (\text{A13})$$

$\forall \tau \neq 0$, Eq. (A13) is Fick's second law of diffusion.

2. The quadratic form of the rate function

It can be shown that the coefficients in Eq. (42) can be written as

$$A_1(\tau) = \left(1 + \frac{r_1}{r_2}\right)^n, \quad (\text{A14})$$

$$A_2(\tau) = \frac{1}{\sqrt{\tau}} \frac{n}{\sqrt{\pi D}} \frac{1}{r_2} \left(1 + \frac{r_1}{r_2}\right)^{n-1}, \quad (\text{A15})$$

$$A_3(\tau) = \frac{n(n-1)}{2D\pi} \frac{1}{\tau r_2^2} \left(1 + \frac{r_1}{r_2}\right)^{n-1}, \quad (\text{A16})$$

$$B_1(\tau) = \left(1 + \frac{r_3}{r_4}\right)^m, \quad (\text{A17})$$

$$B_2(\tau) = \sqrt{\frac{D}{\tau}} \frac{m}{\sqrt{\pi r_4}} \left(\frac{r_3}{r_4} + 1\right)^{m-1}, \quad (\text{A18})$$

$$B_3(\tau) = \frac{m(m-1)D}{2\pi} \frac{1}{\tau r_4^2} \left(\frac{r_3}{r_4} + 1\right)^{m-1}, \quad (\text{A19})$$

where

$$r_1 = \exp\left(-\frac{\tau}{2MD\kappa}\right), \quad r_2 = \operatorname{erf}\left(\frac{1}{2}\sqrt{\frac{\tau}{MD\kappa}}\right), \quad (\text{A20})$$

$$r_3 = \exp\left(-\frac{MD\tau}{2\kappa}\right), \quad r_4 = \operatorname{erf}\left(\frac{1}{2}\sqrt{\frac{MD\tau}{\kappa}}\right). \quad (\text{A21})$$

3. Some integrals

For all $\alpha, \beta \in \mathbb{R}^+$, define the map $I: \mathbb{R} \rightarrow \mathbb{R}$ such that $I[f(z)] = \lim_{L \rightarrow \infty} \int_{-L}^{+L} dz f(z)$. Integration by parts for the following improper integrals yields the closed forms

$$\begin{aligned} I\{[1 - k_1 \operatorname{erf}(\alpha z)][1 + k_2 \operatorname{erf}(\beta z)]\} \\ = \frac{2}{\sqrt{\pi}} k_1 k_2 \left(\frac{\beta}{\alpha} + \frac{\alpha}{\beta}\right) \frac{1}{\sqrt{\beta^2 + \alpha^2}}, \end{aligned} \quad (\text{A22})$$

$$I\{z[1 - k_1 \operatorname{erf}(\alpha z)][1 + k_2 \operatorname{erf}(\beta z)]\} = \frac{1}{2} \left(\frac{k_1}{\alpha^2} - \frac{k_2}{\beta^2}\right), \quad (\text{A23})$$

$$\begin{aligned} I\{z^2[1 - k_1 \operatorname{erf}(\alpha z)][1 + k_2 \operatorname{erf}(\beta z)]\} \\ = \frac{1}{3\sqrt{\pi}} \frac{k_1 k_2}{(\alpha^2 + \beta^2)^{3/2}} \left[\frac{\beta}{\alpha^3} (2\beta^2 + 3\alpha^2) + \frac{\alpha}{\beta^3} (2\alpha^2 + 3\beta^2)\right], \end{aligned} \quad (\text{A24})$$

such that

$$\lim_{L \rightarrow \infty} k_1 = 1, \quad \lim_{L \rightarrow -\infty} k_2 = 1,$$

where we have used

$$I[z e^{-z^2 \beta^2} \operatorname{erf}(z\alpha)] = \frac{\alpha}{\beta^2} \frac{1}{\sqrt{\beta^2 + \alpha^2}}, \quad (\text{A25})$$

$$I[z^3 e^{-z^2 \beta^2} \operatorname{erf}(z\alpha)] = \frac{\alpha}{\beta^4} \frac{2\alpha^2 + 3\beta^2}{2(\alpha^2 + \beta^2)^{3/2}}. \quad (\text{A26})$$

-
- [1] L. Galfi and Z. Rácz, *Phys. Rev. A* **38**, 3151 (1988).
 - [2] J. Kiefer, S. Havlin, H. Taitelbaum, B. Trus, and G. Weiss, *J. Stat. Phys.* **65**, 873 (1991).
 - [3] Z. Koza and H. Taitelbaum, *Phys. Rev. E* **54**, 1040 (1996).
 - [4] A. Schenkel, P. Wittwer, and J. Stubbe, *Physica D* **69**, 135 (1993).
 - [5] G. van Baalen, A. Schenkel, and P. Wittwer, *Commun. Math. Phys.* **210**, 145 (2000).
 - [6] Z. Koza, *J. Stat. Phys.* **85**, 179 (1996).
 - [7] Z. Koza, *Physica A* **240**, 622 (1997).
 - [8] D. Hilhorst, R. van der Hout, and L. A. Peletier, *J. Math. Anal. Appl.* **199**, 349 (1996).
 - [9] S. Cornell, M. Droz, and B. Chopard, *Phys. Rev. A* **44**, 4826 (1991).
 - [10] Z. Jiang and C. Ebner, *Phys. Rev. A* **42**, 7483 (1990).
 - [11] B. Chopard and M. Droz, *Europhys. Lett.* **15**, 459 (1991).
 - [12] S. Cornell and M. Droz, *Physica D* **103**, 348 (1997).
 - [13] M. Araujo, S. Havlin, H. Larralde, and H. E. Stanley, *Phys. Rev. Lett.* **68**, 1791 (1992).
 - [14] H. Taitelbaum, A. Yen, R. Kopelman, S. Havlin, and G. H. Weiss, *Phys. Rev. E* **54**, 5942 (1996).
 - [15] S. Cornell, M. Droz, and B. Chopard, *Physica A* **188**, 322 (1992).
 - [16] S. Cornell and M. Droz, *Phys. Rev. Lett.* **70**, 3824 (1993).
 - [17] M. Araujo, H. Larralde, S. Havlin, and H. E. Stanley, *Phys. Rev. Lett.* **71**, 3592 (1993).
 - [18] Z. Koza and H. Taitelbaum, *Philos. Mag. B* **77**, 1389 (1998).
 - [19] M. Howard and J. Cardy, *J. Phys. A* **28**, 3599 (1995).
 - [20] Y. E. Koo, R. Kopelman, and L. Li, *Mol. Cryst. Liq. Cryst.* **183**, 187 (1990).

- [21] F. Argoul, M. Bazant, and C. Leger, *J. Phys. Chem. B* **103**, 5841 (1999).
- [22] Y. E. Koo and R. Kopelman, *J. Stat. Phys.* **65**, 893 (1991).
- [23] H. Taitelbaum, Yong-Eun Lee Koo, S. Havlin, R. Kopelman, and G. H. Weiss, *Phys. Rev. A* **46**, 2151 (1992).
- [24] H. Taitelbaum, B. Vilensky, A. Lin, A. Yen, Yong-Eun Lee Koo, and R. Kopelman, *Phys. Rev. Lett.* **77**, 1640 (1996).
- [25] A. Yen, Yong-Eun Lee Koo, and R. Kopelman, *Phys. Rev. E* **54**, 2447 (1996).
- [26] P. Ortoleva, *Oscillations and Traveling Waves in Chemical Systems* (Oxford University Press, New York, 1994).
- [27] M. Burger and R. Field, *Oscillations and Traveling Waves in Chemical Systems* (Wiley, New York, 1985).
- [28] J. Murray, *Extended Irreversible Thermodynamics* (Springer, New York, 1993).
- [29] H. Larralde, M. Araujo, S. Havlin, and H. E. Stanley, *Phys. Rev. A* **46**, 6121 (1992).
- [30] P. L. Krapivsky, *Phys. Rev. E* **51**, 4774 (1995).
- [31] J. Mai, I. M. Sokolov, and A. Blumen, *Phys. Rev. Lett.* **77**, 4462 (1996).
- [32] J. Mai, I. M. Sokolov, V. N. Kuzovkov, and A. Blumen, *Phys. Rev. E* **56**, 4130 (1997).
- [33] D. Kessler and H. Levine, *Nature (London)* **394**, 5556 (1998).
- [34] S. Cornell, Z. Koza, and M. Droz, *Phys. Rev. E* **52**, 3500 (1995).
- [35] M. Araujo *et al.*, *Physica A* **221**, 1 (1995).
- [36] M. Z. Bazant and H. A. Stone, *Physica D* **147**, 95 (2000).
- [37] P. M. J. Trevelyan, *Phys. Rev. E* **79**, 016105 (2009).
- [38] J. Magnin, *Eur. Phys. J. B* **17**, 673 (2000).
- [39] A. A. Ovchinnikov and Y. B. Zeldovich, *Chem. Phys.* **28**, 215 (1978).
- [40] V. Kuzovkov and E. Kotomin, *Rep. Prog. Phys.* **51**, 1479 (1988).
- [41] E. Kotomin and V. Kuzovkov, *Modern Aspects of Diffusion-Controlled Reactions* (Elsevier, Amsterdam, 1996).
- [42] J. Casas-Vázquez, D. Jou, and G. Lebon, *Extended Irreversible Thermodynamics* (Springer, New York, 2010).
- [43] M. Al Ghoul and B. C. Eu, *Physica D* **90**, 119 (1996).
- [44] M. Al Ghoul and B. C. Eu, *Physica D* **97**, 531 (1996).
- [45] M. Al Ghoul, *Philos. Trans. R. Soc. London, Ser. A* **362**, 1567 (2004).
- [46] D. Polyanin, *Handbook of Linear PDEs for Engineers and Scientists* (Chapman and Hall, London, 2002).
- [47] B. Chopard, M. Droz, J. Magnin, and Z. Racz, *Phys. Rev. E* **56**, 5343 (1997).
- [48] J. Yaneva, B. Dünweg, and A. Milchev, *J. Chem. Phys.* **122**, 204105 (2005).
- [49] M. Tsige and G. S. Grest, *J. Chem. Phys.* **120**, 2989 (2004).
- [50] M. Al Ghoul, T. Ghaddar, and T. Moukalled, *J. Phys. Chem. B* **113**, 11594 (2009).